# Scattered Light Modeling of the HD 32297 Debris Disk

Sebastian De Pascuale*
*Department of Physics and Astronomy, University of California, LA*

September 3, 2011

**Abstract**

The morphology of circumstellar debris disks provides indirect evidence for the presence of an exoplanet that may be gravitationally interacting with these grains. Resolving the structure of the disk is limited by the low angular size and high-contrast with the star, both challenges which may be overcome by adaptive optics and image processing respectively. This study chooses the relatively bright edge-on disk of HD 32297 as a candidate resolved in K-band scattered light and reduced by the Locally Optimized Combination of Images (LOCI) algorithm. Using Mie scattering theory and radiative transfer, this paper presents a physical model for the scattered light of a proposed single population of 2.2$\mu$m water ice grains as comparable to observations at different wavelengths. These grains are found to form a disk at an inner radius of 146 AU to an outer extent of 235 AU and are within a scale height of 8.3 AU for the assumed nearly edge-on geometry. A single power law for the surface density was not fit to the reduced data as the $\chi^2$ comparison used was limited by the brightness asymmetry noted on both sides of the disk. Characterization of this asymmetry leaves added complexities to a future study, while the best-fit model achieved does lend support to LOCI as a valuable technique in the resolving of circumstellar debris disks.

## 1 Introduction

Investigations in planet formation are served by recently discovered stellar systems that provide the possibility of directly imaging an exoplanet or indirectly inferring its presence from the associated circumstellar disk of grain debris. Current theories of debris disk evolution suggest that there is a disk/planet connection where an early epoch of planet building is followed by the accretion of gaseous atmospheres on those newly formed planets. In this progression, circumstellar environments become increasingly dusty as the original gas-to-dust ratios decline. Collisional erosion then leads to debris, the spatial distribution of which can be gravitationally influenced by co-orbital planetary bodies (Wyatt 2008). Asymmetric morphology apparent in scattered light imagery or the spectral energy distribution (SED) of thermal emission from the disk may serve as evidence for this type of gravitational presence. However, the received light from the debris is dependent on the grain size and consequently samples certain grain populations. This requires imaging across several wavelengths in order to comprehensively determine the structure of a debris disk and the corresponding extrasolar system.

The imaging scenarios introduced are bound to the high-contrast regime in which they are challenged by the high intrinsic star-to-disk contrast ratio and the stellar point spread function, (PSF) a blurring of the image characteristic to the optical system's response to a point signal. Resolving structures on a low angular scale then depends on high angular resolution improved by adaptive optics hardware. From this, a coronagraph is employed along with image processing techniques to increase the contrast so that the disk is detectable. A particular case demonstrated by Lafrenière et. al (2007) uses angular differential imaging, (ADI) which allows a debris disk to rotate separate from a static PSF, and the Locally Optimized Combination of Images (LOCI) algorithm to resolve an exoplanet point source among quasi-static speckle noise. While used extensively for this purpose, this algorithm is not currently applied to the reduction of extended sources because of the unknown full characterization of inherent self-subtraction.

As an exploration of this procedure, the debris disk of the main-sequence A star HD 32297 is an

*Grinnell College, Grinnell, IA 50112

excellent candidate for the application of the LOCI algorithm since it is has a relatively bright edge-on disk. Schneider et. al (2005) first reported the discovery in near-IR of the nearly edge-on disk, estimating the full extent to ∼400 AU and noting a brightness asymmetry in the opposing sides. Optical infrared imaging by Kalas (2005) confirmed this orientation, extended the range of disk emission to ∼1680 AU, and considered the collision of HD 32297 with a clump of interstellar medium (ISM) as the source of these asymmetries, but a collisional avalanche model for the grain dynamics later proposed by Grigorieva et. al (2008) might also serve as an explanation. Later observation by Fitzgerald et. al (2007) and Moerchen et. al (2007) in mid-IR with the combined modeling of the mid-IR image and thermal SED presented by the former suggest an inner boundary of dust somewhere between ∼60-80 AU. Further scattered light observations support this central clearing feature and continue study of the disk's possible interaction with the ISM (Mawet et. al 2009; Debes et. al 2009).

Adding to a varied study of HD 32297, this paper will forward model the K-band scattered light image processed by LOCI in order to interpret the physical structure of the debris disk. If the same grains that are responsible for the K-band scattered light dominate emission at other wavelengths, then the parameters that govern the model should be consistent with literature reports. Likewise, the conformity will also suggest information lost in the central regions of the image due to the self-subtraction of the disk. The demonstration of an acceptable limit and full characterization of these effects is left to future study that may promote LOCI processing as a new tool in the accurate removal of the stellar PSF and speckle noise.

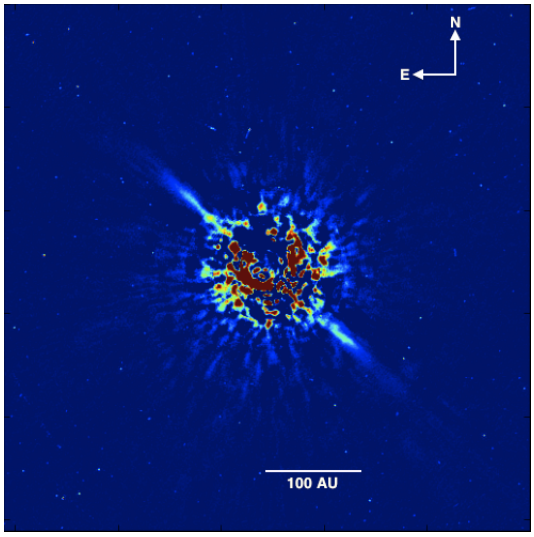


Figure 1: LOCI reduced image in K-band scattered light of the HD 32297 debris disk that will serve as a comparative reference for the three-dimensional model proposed. The image values are scaled to match the model limits and the central regions correspond to excess starlight not blocked during the observation and subtraction artifacts from the LOCI algorithm. The strong NE to SW feature is thought to represent the major axis for a nearly edge-on orientation of the debris disk. This image is used with permission from Esposito et al. (in prep).

# 2 Modeling

A common observational problem in modern astronomy is the inference of three-dimensional structure from objects so distant that only two-dimensional spatial information is possible to obtain. To an observer, these objects are received as an extended two-dimensional image with many sets of parameters that may describe its apparent orientation, structure, density, and brightness at any particular wavelength. In order to estimate these properties, the approach of three-dimensional forward modeling is chosen here over other techniques such as inversion because of the general challenge of noise propagation. This method predicts the specific output of the telescope system given the transfer of radiation through the three-dimensional object to the observer, taking into account the instrumental response. In this way, the model seeks to anticipate the scattered light image of a circumstellar debris disk by constructing a three-dimensional object that translates to a two-dimensional image given a set of parameters specified, assumptions as to the nature of the grain composition and distribution, and the estimated PSF. Therefore, taking these assumptions and varying the parameters may form a best-fit hypothesis to the problem of inferring information of a three-dimensional structure from a two-dimensional image. Depending on the procedure, the set of parameters corresponding to the best-fit may not necessarily be consistent.

## 2.1 *Computational Framework*

This study uses the open source object oriented programming language of Python and several of its modules as the platform of model construction. The Numpy numerical library provides a convenient data structure in the form of arrays, the SciPy scientific distribution contains image processing functions, and the plotting package Matplotlib serves as the visualizer. These tools combine to form a base with a high level of support due to the large community of users.

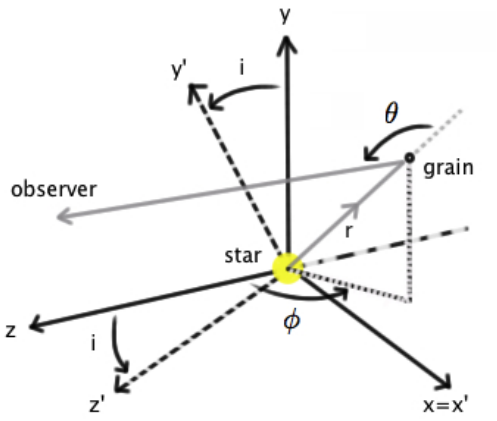


Figure 2: Notations used in this study to describe the orientation of the model disk, the grain distribution, and the light scattered from these grains. Adapted from Augereau et. al (2006).

A three-dimensional data grid is introduced that consists of a set of discrete spatial coordinates set to match the scale of the observational telescope and the resolution of the data. The LOCI reduced image of the HD 32297 debris disk considered here (Fig. 1) is taken in K-band 2.2$\mu$m centered scattered light from the Keck II Telescope Near InfraRed Camera (NIRC2) in the narrow mode with a plate scale of ∼10 mas/pix and with the disk's maximum extent observed at an outer radius of 235 AU.

Line of sight for these observations is considered to be along the $z$-axis in the Cartesian frame $(x, y, z)$ of the three-dimensional model with the star and disk centered at the origin (Fig. 2). A Cartesian frame $(x', y', z')$ is aligned with the disk, where $x = x'$ is the apparent major axis and $y'$ is perpendicular to the disk midplane. Assuming azimuthal symmetry lends a simple transformation to determine the cylindrical frame $(r', \phi', z')$ of the disk.

The relative orientation of the model with respect to the observer may be described in terms of a rotation about the $x$-axis at an angle of inclination, $i$, with $i = 90°$ corresponding to an edge-on disk and the apparent position angle, P.A., of the major axis defined as a two-dimensional rotation about the $z$-axis in the final image.

The HD 32297 debris disk is assumed to be optically thin at all radii such that the grains are considered directly illuminated by the central star at distances $r$ of a disk with a central clearing at $r_{min}$ and a full extent of $r_{max}$. To account for the scattered light, $\theta$ represents the scattering angle with respect to the observer and $\theta = 0$ indicates forward scattering. In this geometry, the stellar distance $d_* \gg r' \gg a$ where $a$ is the grain size or diameter.

## 2.2 *Physical System*

This study is concerned with the physical structure of the debris disk and so the distribution of dust grains may conveniently be described in terms of a total concentration, or number density $n$, of grains as (#/vol). Taking symmetry into consideration, the thin geometry of the disk may define this density function as the product of a two-dimensional (#/area) radial surface density and one-dimensional (1/length) vertical density component where $n(r', z') = \sum(r') \times f(z')$. It is assumed that the surface density follows a power law along the radial extent of the disk and that the vertical density may be described as a Gaussian function to include the scale height, $h$, as another defining parameter in the structure of the debris disk where

$$\sum(r') = \begin{cases} N_o(\frac{r'}{r_{min}})^{\gamma} & \text{for } r_{min} \ll r' \ll r_{max}, \\ 0 & \text{otherwise.} \end{cases} \quad (1)$$

$$f(z') = \frac{2\sqrt{\ln 2}}{h\sqrt{\pi}} e^{\frac{-4z'^2}{h^2 \ln 2}} \quad (2)$$

The radial surface density (1) is normalized to account for a steady-state grain population at $r_{min}$ whose total number is given by $N_o$. Also, the scale height $h = FWHM$ for $f(z')$ (2) so that a smooth distribution is obtained. The total number density $n(r', z')$ is then evaluated at all points within the data grid.

The scattering of light may now be described in terms of the physical properties of these grains. Mie Theory presents the scattering efficiency of homogenous spherical particles where the scattering phase function $P(\theta)$ describes the anisotropic distribution of scattered light. This profile may be treated as the probability distribution of scattered light over all solid angles as a function of the scattering angle, $\theta$ if

$$\int_{4\pi} \frac{P(\theta)}{4\pi} d\Omega = 1 \quad (3)$$

For the K-band image, a population of water ice grains $m = 1.33 - .01j$ on the scale of the wavelength $a = 2.2\mu m$ is assumed. Only single scattering is considered because the debris disk is treated as optically thin. Through the phase function in the single particle case, Mie Theory translates the physical properties of the model system into the quantifiable observable of the scattered light imaged.

To account for the scattering of all grains in the disk, radiative transfer is used. Under this phenomena, the scattered light at a particular frequency is

defined as the brightness, $I_v$, received where conservation of energy holds that $dE_v = I_v dA dt dv d\omega$. The transmission of light from a single grain is the fraction of the total energy received from the star as flux. For a star emitting power or spectral luminosity $L_v^*$, the single grain case is described as

$$I_v = \frac{L_v^*}{4\pi r'^2} \frac{P(\theta)}{4\pi} \tag{4}$$

where the first quantity (4) is the flux received by the grain at a distance $r'$ from the central star. This paper adopts the value $L_k^* = .02 L_{\odot k}$ as calculated from the 2MASS All-Sky Point Source Catalog and Thuillier et. al (2003).

For coherent scattering across multiple grains, consider a volume element containing a number density $n(r', z')$ of grains. The three dimensional emission coefficient $j_v$ defines how the brightness of light changes as it passes through this volume and is presented by a total scattering area

$$j_v = \frac{dI_v}{ds} = I_v n(r', z') \sigma_s \tag{5}$$

where $\sigma_s$ is the scattering cross-sectional area of a single grain. If the line of sight in the direction of the observer is taken to be the $z$-axis (Fig. 2.1) then the total two dimensional brightness as a function of $r'$ that corresponds to the image collected is given by the integral of $j_v$ (5) along $z$ as

$$I_v(r') = \int_{z_1}^{z_2} \frac{L_v^* P(\theta) n(r', z') \sigma_s}{(4\pi r')^2} dz \tag{6}$$

This (6) defines the model image and has 10 degrees of freedom $\{P.A., i, \gamma, N_o, r_{min}, r_{max}, h, L_v^*, a, m\}$ accounting for all parameters assumed within the debris disk system. Note that a strong degeneracy exists in the choice of grain population, $a$, and the rest of the parameters that define the model because the Mie Theory phase function, $P(\theta)$, is particular to the grain size and strongly determines the overall distribution of scattered light.

In reference to the K-band image of HD 32297, the LOCI algorithm worked to subtract the excess starlight and stellar PSF from the data to resolve the structure of the disk. Due to the atmospheric seeing and diffraction limited optics of the telescope, the PSF is also convolved with the image of the disk and therefore must be included in the model. To do this, the PSF may be estimated as a simple Gaussian function on the order of the diffraction limit of the telescope given by the Airy function and angular resolution $R = \lambda(1.22)/D$, where $D$ is the diameter of the aperture. As the PSF corresponds to an extended smoothing of the unresolved disk, this effect of the convolution may be achieved as the product in the spatial frequency domain of the Fourier Transforms of both the PSF and model. The final image is then the inverse transform of this product and gives a model now comparable to the data. For this study, it is assumed that LOCI does not filter the stellar PSF convolved with the debris disk.

## 2.3 *Fitting Procedure*

The two-dimensional model for the scattered light (6) forms the basis for analyzing the debris disk of HD 32297. This model includes assumptions as to the orientation, structure, and density of the disk as well as the parameters that define those properties. As an initial estimate, the system is taken to have a nearly edge-on orientation with the maximum extent of the major axis being the maximum radius from the center of the observed scattered light. Geometrically, this orientation defines the overall two-dimensional projection of the model image and may show dependency with the scale height.

This study seeks to identify the physical structure of the circumstellar debris disk from the resolved K-band scattered light of HD 32297 and therefore leaves the full characterization of the number density as unknown. The functional form of this distribution then presents parameters that may be varied to match the model to the imaged data. Chi-squared analysis is used as the metric of comparison in determining a best-fit

$$\chi^2 = \sum \left( \frac{data - model}{\sigma(r)} \right)^2 \tag{7}$$

where the technique (7) incorporates the standard deviation, $\sigma(r)$, as the noise as a function of the radius from the center of the data image. Conveniently, the constant $N_o$ may be taken to be a normalization of both the starting number of grains in the radial surface power law and the unit conversion difference between the data and model image. This normalization is mathematically chosen to minimize the $\chi^2$ value by differentiating the $\chi^2$ (7) with respect to $N_o$ and setting equal to zero during comparison as

$$N_o = \frac{\sum \frac{2dm}{\sigma(r)^2}}{\sum \frac{2m^2}{\sigma(r)^2}} \tag{8}$$

where $d$ = data and $m$ = model (8).

At this point, the debris disk may be fully characterized by the three unknown parameters left: the power law index, $\gamma$, the inner radius, $r_{min}$, and the scale height, $h$. A three-dimensional parameter space is described by the range of values for each parameter along the three-axes basis of this space.

Each coordinate represents a different model image that may be compared to the reduced data to determine the best-fit combination of these three parameters. However, a search through this space is computationally expensive because the number of three-dimensional models needed is equivalent to the number of coordinates and thus limits the modeling ability to finely sample this space. To reduce the creation time and total memory usage of each model image, this study will consider the average of both sides of the resolved K-band debris disk as the reflection across the vertical and horizontal axes of the reduced image to produce a half-disk average. Actual $\chi^2$ comparison will account only for regions outside of the significantly high $\sigma(r)$ central portion of the disk image. The final procedure then analyzes the region from ∼60-235 AU in both the reduced data and composed model images.

Ranges for the three variable parameters were first chosen according to independent searches through the parameter space for a collection of coordinates in accordance with minimizing the $\chi^2$ value for each parameter individually as if they are independent variables. Once a full search over the selected ranges is complete, the $\chi^2$ analysis results in a three-dimensional space of values that correspond to the three-dimensional parameter space. Taking the coordinate that is associated with the lowest $\chi^2$ value, a single model image may be created to compare with different P.A. rotations of the average data to adjust the angle by further lowering the $\chi^2$. The set of parameters that accounts for this final model image is compiled as the hypothesis for the HD 32297 circumstellar debris disk.

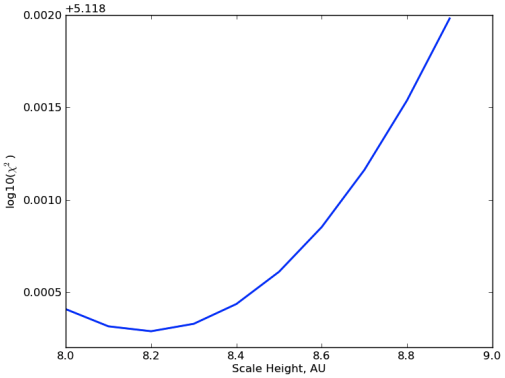


Figure 3: Comparison of the unreduced $\chi^2$ values to the scale height for the range of $60 \leq r_{min} \leq 90$ (AU) and $-3 \leq \gamma \leq 0$ in order to determine an approximate best-fit value at the minimum where $h = 8.2$ AU.

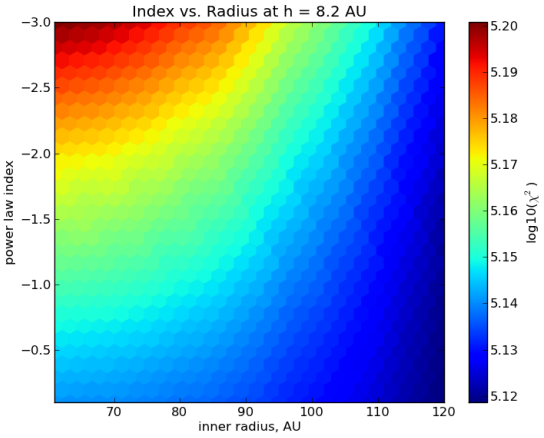


Figure 4: The color map of this plot is scaled logarithmically to the $\chi^2$ values for the coordinates $(r_{min}, \gamma)$ at a fixed $h = 8.2$ AU. Lower values of the $\chi^2$ are taken as indicators of better fit although no best-fit coordinate may be identified.

# 3 Results

Using the scattered light model presented in § 2.2 and following the parameterized search described in § 2.3, the following $\chi^2$ results are obtained for the space defined by the range $60 \leq r_{min} \leq 120$ (AU), $-3 \leq \gamma \leq 0$, $8 \leq h \leq 9$ (AU). After the search of the three dimensional parameter space, a corresponding three dimensional $\chi^2$ space of values associated with those coordinates was generated. To distinguish the results, the best-fit of the scale height $h$ was fixed (Fig. 3) and a slice through the $\chi^2$ space at that value (Fig. 4) was taken to see how the comparison values changed as a function of the other two parameters: the power law index, $\gamma$, and the inner radius, $r_{min}$.

The non-convergent $\chi^2$ trend in this region of the parameter space necessitates another trial that may further bound acceptable values for the power law index and the inner radius. Independent searches of regions further increasing the inner radius identified a potential constraint in the range $140 \leq r_{min} \leq 150$ (AU), $-3 \leq \gamma \leq -2$, $8 \leq h \leq 9$ (AU). A full parameter search of this space revealed

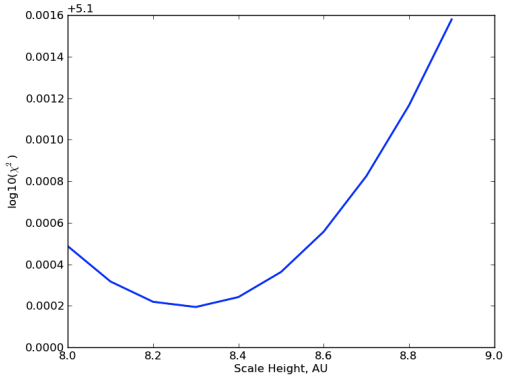


Figure 5: In the range of $140 \leq r_{min} \leq 150$ and $-2 \leq \gamma \leq 0$, the scale height is taken at the minimum where $h = 8.3$ AU.

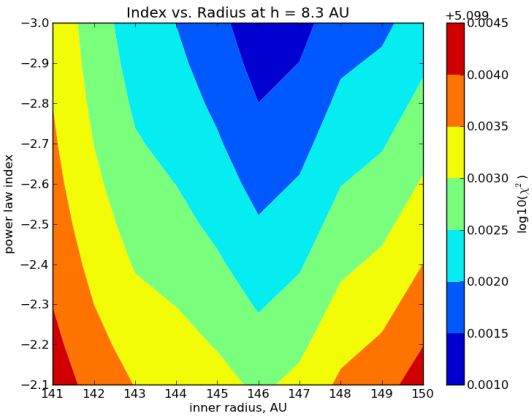


Figure 6: A contour plot is used to better represent this region in the $\chi^2$ space in order to isolate a possible inner radius of best-fit at the minimum $\chi^2$ value.

The final results of the conducted search are given by the assumed static parameters defined in the model creation and the coordinate of variable parameters $(r_{min}, \gamma, h)$ with the lowest $\chi^2$ value. These are collected in the following table

TABLE 1
Best-Fit Model Parameters

| Parameter | Best-Fit | Description |
|---|---|---|
| Static Parameters | | |
| P.A. (deg) | 42.1 | position angle |
| $i$ (deg) | 89 | inclination |
| $r_{max}$ (AU) | 235 | outer edge |
| $\lambda$ ($\mu$m) | 2.2 | wavelength |
| $L_k^*$(erg/s/Hz) | $.02L_{\odot k}$ | stellar luminosity |
| $a$ ($\mu$m) | 2.2 | grain size |
| $m$ | 1.33-.01j | refractive index |
| Variable Parameters | | |
| $\gamma$ | -3 | power law index |
| $N_o$ | 1.8 | $\times 10^{35}$ |
| $h$ (AU) | 8.3 | scale height |
| $r_{min}$ (AU) | 146 | inner edge |

# 4 Discussion

Using the set of resultant parameters, (Table 1) a best-fit model image may be constructed

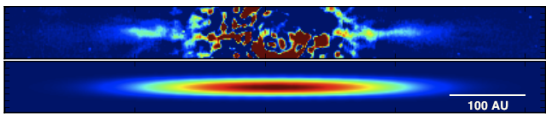


Figure 7: Comparison between the LOCI reduced data (top) and the composed model image (bottom). Note that there are brightness asymmetries on either side of the disk not captured by this simple model.

The model (Fig. 7) captures the overall extent of the debris disk when considered to be nearly edge on. The orientation was estimated as P.A. $= 42.1°$ and $i = 89°$ in attempts to limit the number of unknown parameters and to lower the initial $\chi^2$ fit. These angles are within the uncertainties given by the models of near-IR and mm by Fitzgerald et. al (2007) and Maness et. al (2008) respectively. Note that geometrically, this choice in inclination determined the range of allowed scale heights resulting in a value of $h = 8.3$ AU. For the 2.2$\mu$m grain population considered, the debris disk is modeled to be within the range 146-235 AU for the inner and outer edges respectively. The first observations by Schneider et. al (2005) and Kalas (2005) found the outer extent to be ∼400-1650 AU, much larger than the model because of the wavelength of scattered light imaged. Later modeling by Fitzgerald et. al (2007) and Moerchen et. al (2007) described a central clearing of grains in the inner region ∼60-80 AU of the disk. While the fit between the reduced

data and composed model image are similar in extent, the overestimate of the inner radius is possibly related to the omitted characterization of the brightness asymmetry between the two sides of the disk (Fig. 7), the neglected central regions masked by the noise, and the grain size assumption, which sets the scattering phase function.

Recalling the original search, (Fig. 4) the results in this range exhibit better conformity with the data image for increasing inner radii along which the power law goes from shallow, $\gamma \sim 0$, to steep, $\gamma \sim -3$. The region around $r_{min} \sim 120$ AU marks a transition in the power law index fit. This leads to an unbound value still found in another range, (Fig. 3) which for the sake of the trials conducted is limited to $\gamma = -3$ but is possibly much less according to the method used. In order to quantify the error associated with the $\chi^2$ analysis in terms of the noise present in the sample, a residual map was created that compares the reduced data and final model image as the difference between divided by the standard deviation

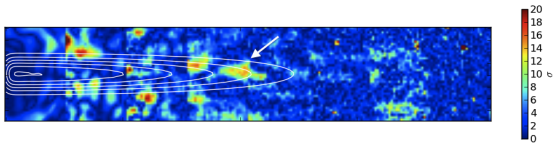


Figure 8: Residual values from the $\chi^2$ comparison. This map represents the subtraction of the data and the model scaled to the level of noise at a particular radius, $\sigma(r)$. The contours of the model image are given as a reference to the spatial extent of the debris disk.

The presence of strong features noted by the arrow (Fig. 8) are $\sim 14\sigma$ in the region 100-120 AU and is most likely associated with the behavior of the power law fit since the divergence occurs in a similar region. It is expected that the observed asymmetry between the two sides of the HD 32297 debris disk is related as the brightness $I_v$ is proportional to the surface number density, which in turn is directly proportional to the power law index, $\gamma$, for a nearly edge-on disk. In comparison, Schneider et. al (2005) found the surface brightness profile, a measure along the major axis of the disk, to have a steep power law for central regions then broken to a shallow power law $\sim$175 AU. The observed wavelengths between this study and the discovery, 2.2$\mu$m and 1.1$\mu$m respectively, may account for this difference. Another factor is the $\chi^2$ technique that in the analysis may fit these features globally with the rest of the data rather than in isolation. Still, this feature may be real and indicates that a power law is not the best model to describe the surface density.

Rather, the brightness asymmetry may be modeled within the overall extent of the disk determined by this study for the 2.2$\mu$m wavelength scattered light. Kalas (2005), Grigorieva et. al (2008), and Debes et. al (2009) have produced different explanations to account for the noted asymmetry. Kalas proposed the collision of the HD 32297 debris disk with a clump of ISM grains as a possibility since the system lies beyond the Local bubble. A later follow up by Debes et. al (2009) to this proposal calculated the relative velocity of the collision and compared HD 32297 with other ISM swept circumstellar debris disks. On the other hand, Grigorieva et. al (2008) determined that the breakup of a planetesimal in the central region of the disk produces a collisional cascade in the density of the system that may also account for the asymmetry. To this, Maness et. al (2008) has traced multiple grain populations in the observed data and even suggests that asymmetries in the mm range may account for grains trapped in resonance with an unseen planetary body.

These studies show that the presence of an exoplanet is not necessarily correlated with a noted asymmetry unless it may be modeled as consistent with the observed data. The large number of observed wavelengths for the HD 32297 debris disk also show that modeling must be consistent across the broad range of data. This incorporates what grain sizes may be considered and what compositions may be explored. In total, an informed picture of a circumstellar debris disk and its associated grain populations may be obtained with a simple model to which complexities are added.

# 5 Summary

This study sought to model the K-band scattered light of the HD 32297 debris disk using $\chi^2$ analysis to compare the constructed model image (6) with the LOCI reduced data (Fig. 1). To conserve time and computer memory, assumptions were made as to the orientation, structure, and composition of the disk leaving only three parameters as unknown quantities to be varied. A search through the parameter space of the ranges of these parameters produced a corresponding $\chi^2$ space of values in which the minimum at a fixed scale height represents the best-fit coordinate $(r_{min}, \gamma, h)$ for the model image. Although no single coordinate gave a best-fit, first estimates for those parameters were obtained.

The purpose of this paper, then, is to provide a physical interpretation, or hypothesis, of the

K-band HD 32297 debris disk by forward modeling the three-dimensional structure from a two-dimensional image. The success of this task may be determined in comparison with literature reports and careful considerations of the assumptions made. Lastly, resources limit the extent to which a study may explore and so balance between the computational aspect and physical aspect of the model is key.

Using Mie Theory to describe the K-band scattered light, this study has found: (1) That for a nearly edge-on orientation, this population is isolated in the region between 146-235 AU and within a scale height of $h = 8.3$ AU. (2) A single power law index was not found that could account for the total structure. (3) Instead, the noted brightness asymmetry should be modeled as the source of the divergent $\chi^2$ analysis.

The opportunity for this research would not have been possible without the guidance of Professor Mike Fitzgerald and the collaboration with graduate student Tom Esposito. Likewise, many of the UCLA Department of Physics and Astronomy faculty contributed to the overall experience. In particular, the author of this paper would like to specially acknowledge Francoise Queval as the proponent for the organization of this Research Experience for Undergraduates (REU) program and the continual support of science as funded by the National Science Foundation (NSF).

## References

Augereau, J.-C., & Beust, H., 2006, A&A, 455, 987

Debes, J. H., Weinberger, A. J., & Kuchner, M. J. 2009, ApJ, 702, 318

Esposito, T., et al. 2011, in preparation

Fitzgerald, M. P., Kalas, P. G., & Graham, J. R. 2007b, ApJ, 670, 557

Grigorieva, A., Artymowicz, P., & Thébault, Ph. 2008, A&A, 461, 537

Kalas, P. 2005, ApJ, 635, L169

Lafrenieère, D., Morois, C., Doyon, R., Nadeau, D., & Artigau, É. 2007, ApJ, 660, 770

Maness, H. L., Fitzgerald, M. P., Paladini, R., Kalas, P., Duchene, G., & Graham, J. R. 2008, ApJ, 686, L25

Mawet, D., Serabyn, E., Stapelfeldt, K., & Crepp, J. 2009, ApJ, 702, L47

Moerchen, M. M., Telesco, C. M., De Buizer, J. M., Packham, C., & Radomski, J. T. 2007, ApJ, 666, L109

Schneider, G., Silverstone, M. D., & Hines, D. C. 2005, ApJ, 629, L117

Thuillier, G., Hersé, M., Labs, D., Foujols, T., Peetermans, W., Gillotay, D., Simon, P. C., & Mandel, H. 2003, Sol. Phys., 214, 1

Wyatt, M. C. 2008, ARA&A, 46, 339